Science Bulletin 69 (2024) 2332–2336

Contents lists available at ScienceDirect

Science Bulletin

journal homepage: www.elsevier.com/locate/scib

Short Communication

Chelation strategy induced blue-shift for efficient deep-blue perovskite light-emitting diodes

Yu Xia [a,1], Zhipeng Zhang [b,1], Yu-Hang Zhou [a], Yu-Han Li [a], Bin Wang [a], Kai-Li Wang [a], Chun-Hao Chen [a], Jing Chen [a], Ilhan Yavuz [c], Guichuan Xing [b], Zhao-Kui Wang [a,*]

[a] Institute of Functional Nano & Soft Materials (FUNSOM), Jiangsu Key Laboratory of Advanced Negative Carbon Technologies, Jiangsu Key Laboratory for Carbon-Based Functional Materials & Devices, Soochow University, Suzhou 215123, China
[b] Joint Key Laboratory of the Ministry of Education, Institute of Applied Physics and Materials Engineering, University of Macau, Macao 999078, China
[c] Department of Physics, Marmara University, Ziverbey, Istanbul 34722, Turkey

ARTICLE INFO

Article history:
Received 7 March 2024
Received in revised form 14 April 2024
Accepted 27 May 2024
Available online 31 May 2024

Metal halide perovskite, regarded as a potential material for next-generation display and lighting applications, has attracted great attention [1,2]. The development of blue perovskite light-emitting diodes (PeLEDs) remains stagnant compared with their green and red counterparts in recent years [3–8]. Meanwhile, among the emitters of different blue emission regions, the development of deep-blue PeLEDs urgently required by the display application lagged significantly behind. Therefore, conducting research on deep-blue PeLEDs (<460 nm) to achieve the desired color gamut in the range of the Commission Internationale de l'Eclairage (CIE) color coordinates approaching (0.131, 0.046) that fulfill the Rec. 2020 specification holds paramount importance. However, obtaining deep-blue emission in perovskites through the straightforward implementation of the common strategies involving excessive chloride incorporation and dimensional reduction presents a significant challenge.

Previous work has demonstrated that guanidine cation (GA) could induce deep-blue emission through stabilizing low-dimensional domains in quasi-two-dimensional (2D) perovskite [9]. Herein, our work focuses on the investigation of mechanisms regarding this. In detail, employing GA as a chelating agent, the binding of the precursor to the surface of bulk perovskites is inhibited, effectively suppressing the formation of large-*n* domains. As shown in Fig. 1a, b, the PeLEDs were constructed with the widely reported device structure of indium tin oxide (ITO)/poly(*N*-vinyl carbazole) (PVK)/perovskite/TPBi/Liq/Al. As Fig. 1c–e shows, with the introduction of chelating agent GA, the obtained deep-blue PeLED exhibited electroluminescence (EL) emission located at about 458 nm with a maximum luminance of 55.16 cd cm^{-2} and an external quantum efficiency (EQE) of 5.65% in the champion device. In contrast, the PeLED without GA delivered initial pure-blue emission at about 474 nm with a peak EQE of 9.34% and a maximum luminance of 96.51 cd cm^{-2} (Fig. S1 online). The obtained deep-blue device delivered a spectrally stable deep-blue emission with corresponding CIE coordinates of (0.140, 0.068) displayed in Fig. S2 (online). No apparent EL spectral shift could be observed from Fig. 1e and the corresponding CIE coordinates remained constant (Fig. 1f) under an increasing forward bias up to 7.0 V, exhibiting excellent spectral stability. The EQE histogram from 20 fabricated deep-blue devices (Fig. 1g) reflected a standard Gaussian distribution with an average EQE of 4.64%, demonstrating superior reproducibility of this strategy. The operational lifetime of the target PeLEDs under a constant current density (1 mA cm^{-2}) was recorded in Fig. 1h. A half-lifetime (T_{50}, time when the luminance decays to half of its initial value) of 12.35 min with an initial luminance of 17.8 cd m^{-2} was realized in the deep-blue device. In contrast to prior advances summarized in Fig. 1i, the maximum EQE of 5.65% reported here is a considerable performance among all types of PeLEDs in the wavelength region from 440–460 nm [9–18].

We carried out a series of characterizations to investigate the mechanism behind it. For the convenience of distinction, the quasi-2D perovskite films without GA were designated as "Pristine". Similarly, the obtained film with deep-blue emission was marked "With GA". The steady-state photoluminescence (PL) and ultraviolet-visible (UV–Vis) absorption measurement were first employed to evaluate the optical properties (Figs. S3 and S4 online). It was preliminarily reasonable to infer that the incorpora-

* Corresponding author.
E-mail address: zkwang@suda.edu.cn (Z.-K. Wang).
[1] These authors contributed equally to this work.

https://doi.org/10.1016/j.scib.2024.05.045

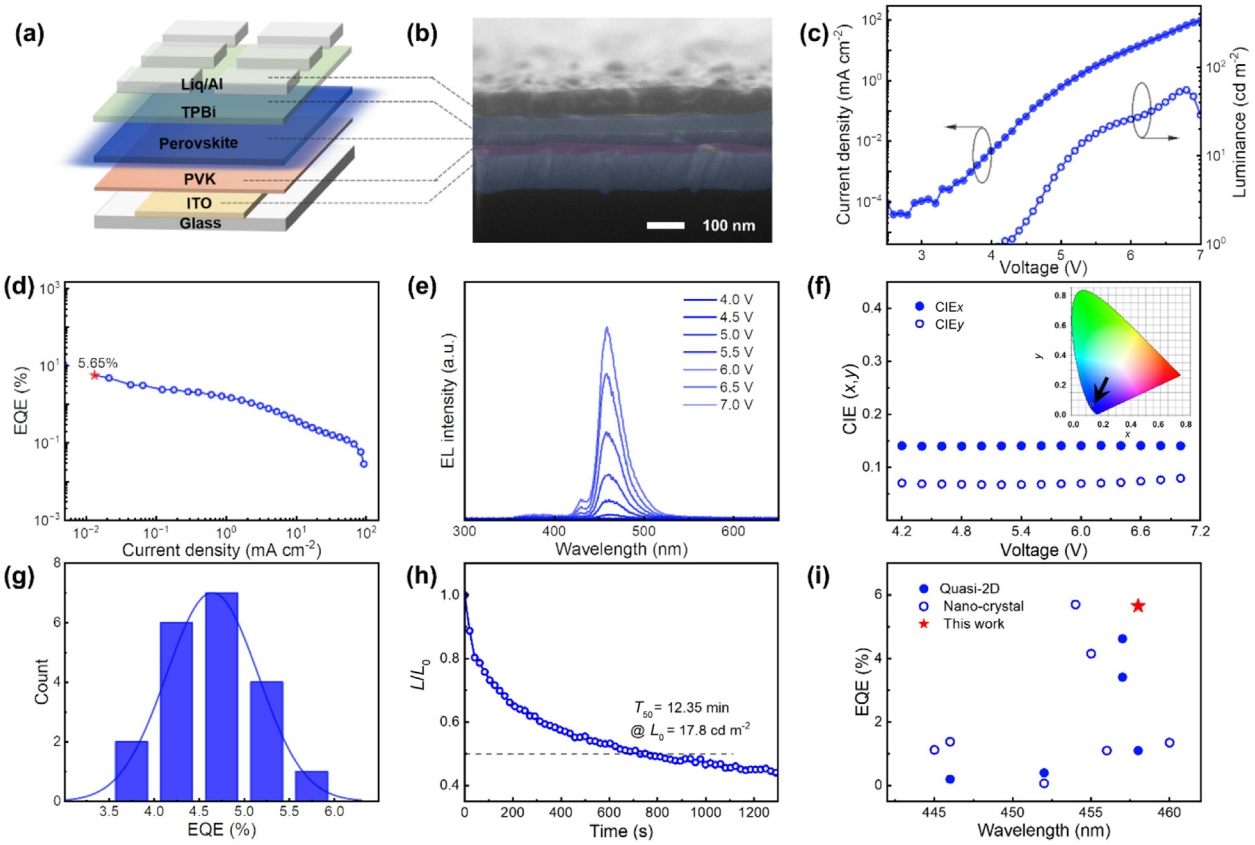

Fig. 1. Device structure and performance of the deep-blue PeLED. (a) Schematic architecture of PeLEDs. (b) Cross-sectional scanning electron microscopy (SEM) image of PeLEDs. (c) Current density–voltage and luminance-voltage curves of the deep-blue PeLEDs. (d) EQE-current density curve of the deep-blue device. (e) EL spectra under different bias voltages. (f) CIE coordinates under different bias voltages. Inset is the corresponding CIE coordinates. (g) Histogram of peak EQEs measured from 20 devices. (h) T_{50} lifetime measurements for deep-blue devices under a constant current density of 1 mA cm^{-2}. (i) Comparison of our work with previous deep-blue PeLED results with emissions ranging from 440 to 460 nm.

tion of GA enabled deep-blue emission by inducing the formation of low-dimensional domains with larger band gaps. In addition, the energy levels of both perovskite films were determined in Fig. S5 (online) by combining ultraviolet photoelectron spectroscopy (UPS) results. The obtained corresponding energy level diagram of both devices was plotted in Fig. S6 (online).

We divided the whole process into five stages for a more intuitive investigation (Supplementary Materials Note 1 online). It could be seen from the X-ray diffraction (XRD) patterns in Fig. S7 (online) that both films exhibited a transition from low-dimensional to high-dimensional structure. From the PL spectra of pristine film (Fig. S8a online), the transformation from the small-n (n represents the number of PbX_6 inorganic layers between two organic layers) domain to the large-n domain during the crystallization process was demonstrated. However, this transformation was not distinct in the film with GA (Fig. S8b online). Fig. S9 (online) extracted the specific content of the n = 2 domain at different stages in both perovskite films. A similar trend (a less distinct red-shift during the crystallization process in the GA sample) could also be observed from the absorption spectra of different stages in Fig. S10 (online). The temperature-dependent PL measurements at the temperature region from 80 to 300 K were recorded in Fig. S11 (online). Over nearly the entire temperature range, an increased exciton peak intensity corresponding to the n = 2 domain was observed in the film with GA. The fitted E_b value of the perovskite film with GA was 140 meV, which was larger than that of the pristine film (Fig. S12 online). The larger exciton binding energy revealed a stronger confinement effect, which was consistent with the increased content of the low-dimensional domain in perovskite film with GA. The higher content of the n = 2 domain in the perovskite film with GA was also further substantiated by the higher exciton peak intensity from the PL excitation spectra in Fig. S13 (online). Transient absorption (TA) pump–probe spectroscopy measurements were then employed to investigate the difference of energy transfer processes (Figs. S14 and S15 online). It was demonstrated that the film with GA displayed a relatively slower cascade energy transfer, which would lead to charge accumulation and recombination in the small-n domains (i.e., n = 3) rather than the large-n domains (i.e., $n \geq 4$). More contribution of the small-n domain to the luminescence facilitated the possibility to realize the deep-blue emission in the film with GA.

As the extensively reported A-site cations, GA was revealed here for the first time to have the potential to realize deep-blue emission. In addition, formamidinium cation (FA), another A-site cation, was employed to passivate defects in our quasi-2D system. We prepared perovskite films with only one cation employed and performed corresponding absorption and PL measurements (Fig. S16 online). From Fig. S16 (online), we suspected that both FA and GA cations may have the ability to induce a blue-shift of emission. It was confirmed by EL measurement of 3D perovskite devices with different concentrations of FA/GA (Fig. S17 online), both FA and GA can induce a significant blue-shift of the EL spectra. However, the introduction of excess FA led to a serious disorder of the EL spectra with the appearance of additional acromions and the abrupt increase of full-width-at-half-maximum (FWHM) (Fig. S18 online). We attributed it to the FA-induced wide domain distribution,

which was consistent with the PL and absorption spectra. By contrast, excessive GA incorporation could only lead to the slight deterioration of the optical properties (Fig. S19 online) with no fatal consequences concerned, demonstrating its superiority to FA in inducing the blue-shift of EL emission.

We seek to give a reasonable explanation for the mechanism. It was demonstrated that GA and FA cations were confined in the vicinity of perovskite (just like the p-F-PEA cations) rather than occupying the A-site in the perovskite lattice since no extra diffraction peaks and lattice strains were observed from the XRD patterns (Fig. S20 online). To further confirm this conclusion, we conducted the XRD measurements of 3D perovskite with different concentrations of FA added (Fig. S21 online). We speculated that GA, as a chelating agent, had a chelation interaction with the precursor to control the growth dynamics of the quantum well during crystallization. The chelation between the precursor ($PbBr_2$) and the chelating agent was directly confirmed by liquid-state ^1H nuclear magnetic resonance (^1H NMR) as shown in Fig. S22 (online). In addition, the shift of absorption feature from 1565 to 1549 cm^{-1} corresponding to the in-plane bending vibration (δ(N–H)) in Fourier transform infrared spectroscopy (FTIR) also contributed to the demonstration of chelation (Fig. S23 online). Combined with the experimental results mentioned above, we believed that GA chelating agent stabilized the low-dimensional domain through the chelation with the lead precursor. The mechanism diagram of GA chelating agent stabilizing low-dimensional domains during crystallization was illustrated in Fig. 2a. In the initial stage of nucleation, the formation of n = 1 low-dimensional domain was much more favorable due to the strong van der Waals interaction between the spacer cations. In the pristine perovskite film, the low-soluble Cs cation could easily occupy the A-site due to the higher tendency to reach supersaturation and induce the subsequent attachment of lead precursors on the bulk perovskite structure, accounting for the transformation from the small-n domain to the large-n domain as shown in PL spectra. While in the film with GA, the tendency of lead precursors to be chelated by the GA chelating agent in the vicinity of bulk perovskite inhibited its binding to the perovskite surface, thereby suppressing the growth of large-n domains. Therefore, no evident domain transformation was observed in the film with GA.

We expected to explore similar alternative chelating agents to realize deep-blue emission in the quasi-2D perovskite. To demonstrate the universality of this chelate-assisted strategy, another widely reported ethylamine cation (EA) anticipated to be a new alternative chelating agent was proposed (Fig. 2b). They differed in the number of hydrogen bonds they could generate with lead

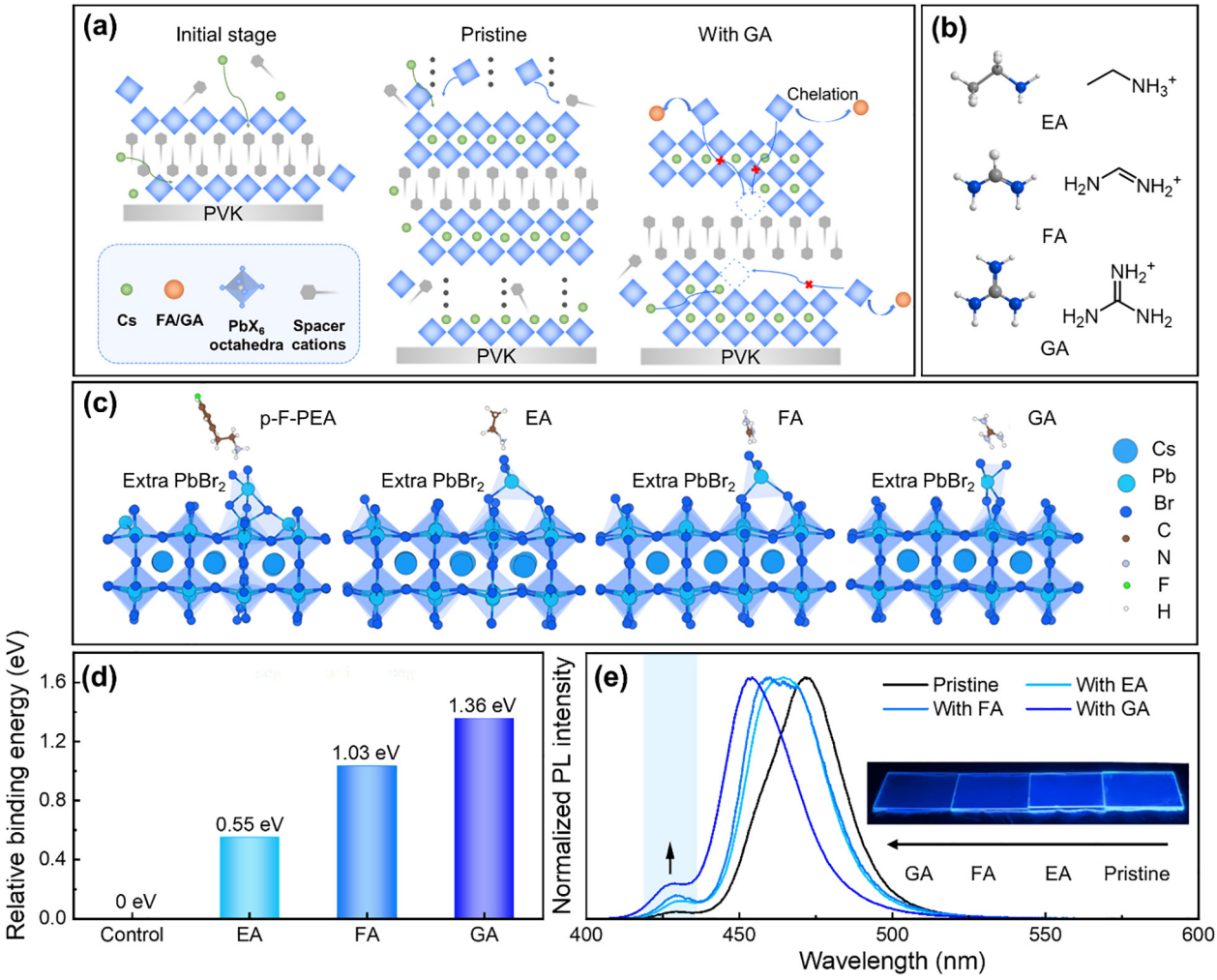

Fig. 2. The universality of chelate-assisted strategy for efficient domain distribution management. (a) The schematic diagram of chelate-assisted strategy for stabilized low-dimensional domains to realize deep-blue emission. (b) Molecular structure of the EA/FA/GA chelating agents. (c) Schematic of the binding of $PbBr_2$ on the surface of perovskite under the influence of different chelating agents nearby. (d) DFT-calculated relative binding energy of $PbBr_2$ on the surface of perovskite. As a control, the binding energy of $PbBr_2$ on the perovskite surface was defined as 0 eV when p-F-PEA cations were nearby. (e) PL spectra of pristine perovskite film and perovskite films with the same amount of different chelating agents. Inset is the photograph of the perovskite films under external photoexcitation.

precursors, which had a direct impact on the chelation tendency. Corresponding absorption and PL measurements of the EA only perovskite film were supplemented in Fig. S24 (online). Density functional theory (DFT) calculations were employed to further quantify the chelation magnitude. We calculated the relative binding energy of $PbBr_2$ on the surface of bulk perovskite under the influence of different chelating agents nearby (Fig. 2c and Supplementary materials Note 2 online). The calculated relative binding energies were 0.55, 1.03, and 1.36 eV for EA, FA, and GA system respectively as shown in Fig. 2d. The increased relative binding energy from EA to FA to GA stood for the gradually weaker binding of $PbBr_2$ to the surface of bulk perovskite, so attachment of the excess $PbBr_2$ became less likely. The gradual increase in the exciton peak intensity corresponding to the n = 2 domain was observed in the PL spectra (Fig. 2e), further validating our conclusion. The EL spectra of the corresponding devices we fabricated in Fig. S25 (online) also exhibited a consistent trend. In addition, another similar chelating agent (Biguanide cation, BC) was also demonstrated to promote the formation of more low-dimensional domains from the PL spectra (Fig. S26 online). We emphasize the superiority of this strategy in realizing the deep-blue emission to the conventional composition and dimensional engineering. As presented in Fig. S27 (online), same amounts of CsCl and p-F-PEABr were added to the precursor solution with the expectation of achieving an equivalent blue-shift of the EL emission in the fabricated device. It was impractical to realize deep-blue emission of quasi-2D perovskites through conventional composition and dimensional engineering, demonstrating the superiority of our chelate-assisted strategy in contrast.

In summary, we first revealed the mechanism by which GA stabilized low-dimensional domain during the crystallization process. We successfully fabricated a spectrally stable deep-blue perovskite emitter emitting at 458 nm with a remarkable EQE of 5.65%. Furthermore, the universality of different chelating agents in efficiently managing domain distribution to achieve a blue-shift in EL emission was also demonstrated, providing more considerable alternatives for the ultimate realization of deep-blue emission. Our findings present a promising third pathway to attain deep-blue emission, surpassing the limitations of excessive chloride incorporation and dimensional reduction commonly employed in conventional methods.

Conflict of interest

The authors declare that they have no conflict of interest.

Acknowledgments

This work was supported by the National Natural Science Foundation of China (62075148, 52073197, and 52273189), the Natural Science Foundation of Jiangsu Province (BE2022026-2, BK20201413, BK20211314), Suzhou Science and Technology Plan Project (N321461821, ST202212), Suzhou Key Laboratory of Functional Nano & Soft Materials, Collaborative Innovation Center of Suzhou Nano Science & Technology, the 111 Project, and Joint International Research Laboratory of Carbon-Based Functional Materials and Devices.

Author contributions

Yu Xia and Zhao-Kui Wang conceived the idea. Yu Xia fabricated the devices and designed the experiments. Zhipeng Zhang performed the TA measurement under the supervision of Guichuan Xing. Ilhan Yavuz performed the DFT calculation. DFT calculations are performed in the UHEM computing cluster of Istanbul Technical University, Turkey. Yu-Hang Zhou, Yu-Han Li, Bin Wang, Kai-Li Wang, Chun-Hao Chen, and Jing Chen assisted with the characterizations. Yu Xia and Zhao-Kui Wang wrote the manuscript. All the authors discussed the results and commented on the manuscript. Zhao-Kui Wang supervised the project.

Appendix A. Supplementary materials

Supplementary materials to this short communication can be found online at https://doi.org/10.1016/j.scib.2024.05.045.

References

[1] Liu S, Guo Z, Wu X, et al. Zwitterions narrow distribution of perovskite quantum wells for blue light-emitting diodes with efficiency exceeding 15%. Adv Mater 2023;35:2208078.
[2] Zhang F, Zhong H, Chen C, et al. Brightly luminescent and color-tunable colloidal $CH_3NH_3PbX_3$ (X= Br, I, Cl) quantum dots: Potential alternatives for display technology. ACS Nano 2015;9:4533–42.
[3] Ma D, Lin K, Dong Y, et al. Distribution control enables efficient reduced-dimensional perovskite LEDs. Nature 2021;599:594–8.
[4] Sun Y, Ge L, Dai L, et al. Bright and stable perovskite light-emitting diodes in the near-infrared range. Nature 2023;615:830–5.
[5] Jiang Y, Sun C, Xu J, et al. Synthesis-on-substrate of quantum dot solids. Nature 2022;612:679–84.
[6] Chen F, Liu Y, Zhang D, et al. Bilayer phosphine oxide passivation toward efficient and large-area pure-blue perovskite quantum dot light-emitting diodes. Sci Bull 2023;68:2354–61.
[7] Shen W, Liu Y, Grater L, et al. Thickness-variation-insensitive near-infrared quantum dot LEDs. Sci Bull 2023;68:2954–61.
[8] Yu H, Chen W, Fang Z, et al. Alkalis-doping of mixed tin-lead perovskites for efficient near-infrared light-emitting diodes. Sci Bull 2022;67:54–60.
[9] Zhou Y, Wang C, Yuan S, et al. Stabilized low-dimensional species for deep-blue perovskite light-emitting diodes with EQE approaching 3.4%. J Am Chem Soc 2022;144:18470–8.
[10] Wang L, Shi Z, Ma Z, et al. Colloidal synthesis of ternary copper halide nanocrystals for high-efficiency deep-blue light-emitting diodes with a half-lifetime above 100 h. Nano Lett 2020;20:3568–76.
[11] Zou G, Li Z, Chen Z, et al. Color-stable deep-blue perovskite light-emitting diodes based on organotrichlorosilane post-treatment. Adv Funct Mater 2021;31:2103219.
[12] Deng W, Xu X, Zhang X, et al. Organometal halide perovskite quantum dot light-emitting diodes. Adv Funct Mater 2016;26:4797–802.
[13] Song J, Li J, Li X, et al. Quantum dot light-emitting diodes based on inorganic perovskite cesium lead halides ($CsPbX_3$). Adv Mater 2015;27:7162–7.
[14] Zhang M, Bi C, Xia Y, et al. Water-driven synthesis of deep-blue perovskite colloidal quantum wells for electroluminescent devices. Angew Chem Int Ed 2023;62:e202300149.
[15] Zhang B, Yuan S, Ma J, et al. General mild reaction creates highly luminescent organic-ligand-lacking halide perovskite nanocrystals for efficient light-emitting diodes. J Am Chem Soc 2019;141:15423–32.
[16] Dong J, Lu F, Han D, et al. Deep-blue electroluminescence of perovskites with reduced dimensionality achieved by manipulating adsorption-energy differences. Angew Chem Int Ed 2022;134:e202210322.
[17] Liu H, Shonde T, Olasupo O, et al. Organic semiconducting ligands passivated $CsPbBr_3$ nanoplatelets for blue light-emitting diodes. ACS Energy Lett 2023;8:4259–66.
[18] Qin Z, Wang S, Zhu Y, et al. Co-regulation strategy dominated by double short molecules permitting the regrowth of quantum dots for efficient deep-blue perovskite light-emitting diodes. Nano Energy 2024;121:109263.

Yu Xia is now a Ph.D. student of materials science and engineering under the supervision of Prof. Zhao-Kui Wang at Functional Nano & Soft Materials Laboratory of Soochow University, China. He received his B.S. degree from Soochow University in 2021. His research interest mainly focuses on efficient perovskite light-emitting diodes.

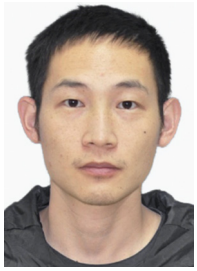

Zhipeng Zhang received his bachelor's degree from Nanjing Tech University in 2015 and his Ph.D. degree from University of Macau in 2022. He is now worked as a postdoctoral researcher at the Institute of Applied Physics and Materials Engineering of University of Macau. His current research interest is developing novel halide perovskite single crystals and nanocrystals, and the charge carrier dynamics in perovskite materials.

Zhao-Kui Wang received his Ph.D. degree in nano and novel matter science from the University of Toyama, Japan, in 2011. After working at the University of Toyama as a JSPS research fellow from 2011–2013, he joined the Institute of Functional Nano & Soft Materials (FUNSOM), Soochow University, as an associate professor. Since 2017, he has been a full professor at Soochow University. His main research interest lies in organic and inorganic/organic hybrid materials and devices, focusing on solar cells and light-emitting diodes.